

Chemical Heterogeneity of a Large Cluster IDP: Clues to its Formation History Using X-ray Fluorescence Mapping and XANES Spectroscopy S. Wirick¹, G. J. Flynn², S. Sutton^{1,3}, M. E. Zolensky⁴,¹ Center for Advanced Radiation Sources, Univ. of Chicago, Chicago, IL 60637, USA, (swirick@bnl.gov), ²Dept. of Physics, Plattsburgh University NY 12901, USA, ³ Dept of Geophysical Sciences, Univ. of Chicago, Chicago IL 60637, USA, ⁴NASA Johnson Space Center, Houston, TX, 77058, USA

Introduction: Chondritic porous IDPs may be among the most primitive objects found in our solar system [1]. They consist of many micron to submicron minerals, glasses and carbonaceous matter [2,3,4,5,6,7] with > 10⁴ grains in a 10 μm cluster [8]. Speculation on the environment where these fine grained, porous IDPs formed varies with possible sources being pre-solar dusty plasma clouds, protostellar condensation, solar asteroids or comets [4,6,9]. Also, fine grained dust forms in our solar system today [10,11]. Isotopic anomalies in some particles in IDPs suggest an interstellar source[4,7,12]. IDPs contain relic particles left from the dusty plasma that existed before the protostellar disk formed and other grains in the IDPs formed later after the cold dense nebula cloud collapsed to form our protostar and other grains formed more recently. Fe and CR XANES spectroscopy is used here to investigate the oxygen environment in a large (>50 10 μm or larger sub-units) IDP.

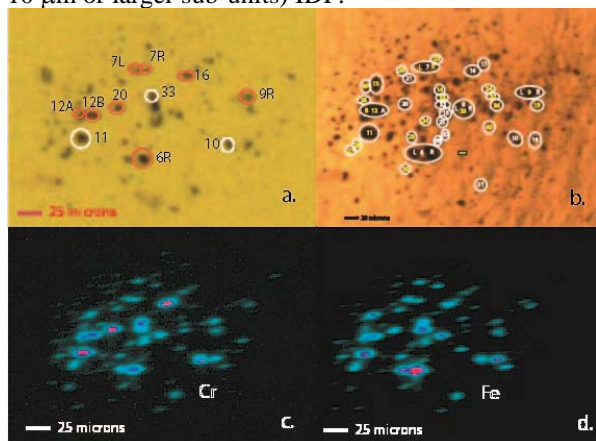


Figure 1. a. transmitted visible light image, b.reflected visible light image, c. Cr fluorescence map d. Fe fluorescence map.

Sample and Analysis: Cluster particle L2009R2 cluster #13 is a chondritic, porous IDP, inferred to be extraterrestrial from its high Ni/Fe. The cluster is spread over an area approximately 250 μm in size and the collection silicon oil is still present (Fig.1b). The IDP is mounted on 7 μm thick Kapton film. Using the X26A microprobe beamline at the National Synchrotron Light Source (Brookhaven Nat. Lab.) 55 areas were analyzed using: 2D X-ray microdiffraction; Fe and Cr X-ray Absorption Near Edge Structure (XANES) spectroscopy and X-ray fluorescence fly-scan mapping at 7.2 and 13.5 keV. Cr and Fe XANES spectra were col-

lected every 5 μm, approximately covering the 250 μm box and all of the spectra were summed to determine the average oxidation state of the Fe and Cr species [8]. Cr XANES spectra were also collected where the Cr concentrations were high enough to produce low-noise spectra. Only 11 areas, circled in Fig.1a were used to collect Cr XANES spectra. EDX data from Johnson Space Center (JSC) Curatorial facility on a ~10μm size aggregate from this large cluster contained Mg, Al, Si, S, Ca, Cr, Fe and Ni. The SEM image of this fragment shows many submicron size grains.

Results: XRD: Of the 55 areas were 2D diffraction data were collected only 25 areas recorded Bragg reflections (yellow areas Fig 1b). In the areas where no Bragg reflections (amorphous) were detected there may be submicron crystalline material not detected due to the detection limits of the diffraction setup. Of the 11 areas analyzed here 3 were amorphous.

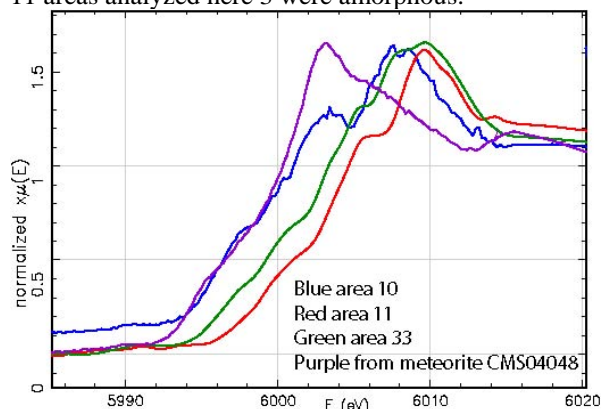


Figure 2. Cr XANES spectra from L2009R2 cluster #13 area 10, 11,33 compared to Cr XANES spectra from an olivine in ureilite CMS04048.

Cr-XANES: Fig. 2 shows Cr XANES from 3 of the 11 areas where spectra were collected. The spectra plotted span the range of oxidation for Cr in L2009R2 cluster #13 with spectra from areas 6R, 7R, 7L, 9R, and 16 nearly over plotting with spectra from area 11, chromite and diopside also plot here. For areas 12A,12B, and 20 the spectra have more reduced Cr, lying closer to the spectrum from area10. Also plotted in Fig.2 is a Cr spectrum from an olivine from ureilite CMS04048 with a Cr oxidation state of 2.22 (Sutton, S., et al. submitted).

Fe-XANES: Fig. 3 contains Fe XANES spectral plots from L2009R2 cluster #13 which also show variability

in the Fe oxidation state with the blue plot representing metallic Fe or Fe-Ni and the spectrum from area 7R plotting near pyrrhotite. The other spectra vary around area 7R's spectrum and are more or less oxidized.

XRF: X-ray fluorescence spectra were collected by integrating the pixel data from a defined region in the flyscan data set. Besides Cr, all 11 areas contain Mn, Fe, Ni, Cu and Zn. Calcium is present in all but 2 areas (area 6R and 7L) and Cl is found in areas 9R and 10. Area 10 is also the area with the most reduced

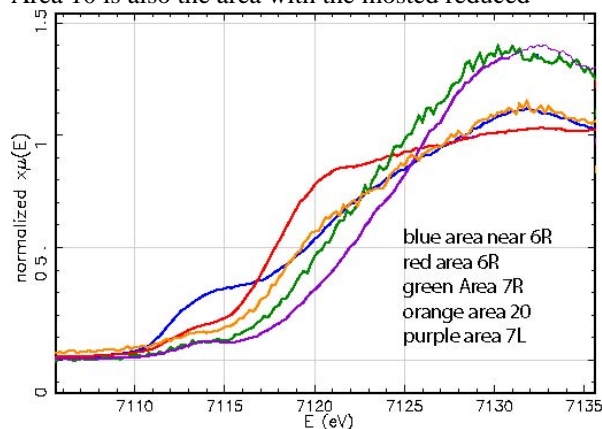


Figure 3. Fe XANES spectra from L200R29 cluster #13 areas 6R, 7L, 7R, and 20.

form of Cr. Below 3 keV the fluorescence yield is low for data collected at 13.5 keV, S is only seen in a few spectra and the peaks are small. S peaks were also small for data collected at 7.2 keV. There may also be matrix effects resulting in reduced S peaks. Area 6R also contained Se. This was the only area where Se was found. Future work will include longer collection time to improve the signal to noise which will increase our ability to detect lower concentrations. Zn/Fe ratios normalized to CI for all 11 areas were around 5 suggesting there was no loss of moderately volatile elements such as Zn upon atmospheric entry.

Discussion: Both the Cr and Fe XANES spectra span a large range in the oxidation state of these 2 elements suggesting environments with varying O₂ concentrations when these various species found in the 10 μm sub-units of this large cluster IDP formed. The relatively high Zn/Fe normalized to the CI Zn/Fe ratio suggests this cluster particle was not significantly heated upon atmospheric entry and likely did not oxidize much before being collected. Others have found heterogeneity in small CP IDPs [2,3,4,5,6,7,8,9,12] using EDX elemental analysis, isotopic analysis, and mineral identification but only Flynn et al [8] have used both Cr and Fe XANES spectroscopy to characterize oxidation state of large (>150 μm) IDPs. The XANES spectral data can be used to determine the oxidation state of the element of interest. For grain

collections such as those found in large cluster IDPs, where it is possible the minerals are grown from gas phase and not melt conditions one could generate theoretical redox buffer curves for Cr using thermodynamic data for known oxide forms [13]. This plot would assume a system in equilibrium using ideal/simple components so laboratory experiments would be needed to confirm how applicable this plot would be when applied to IDPs. The most reduced form of Fe is found in area 6R while the Cr XANES spectra from area 6R is best represented by Chromite or Diopside with an oxidation state of 3+. The most reduced form of Cr (oxidation state 2+) is found in area 10 and the Fe XANES spectrum from this area is best represented by pyrrhotite. Even comparison of Fe XANES spectra from area 7R and 7L shows a difference in the Fe oxidation state. These areas are ~10 μm apart.

Conclusions: Analyzing large (>50 10 μm or larger sub-units) CP IDPs gives one a view on the environments where these fine dust grains formed which is different from that found by only analyzing the small, 10 μm IDPs. As with cluster IDP L2008#5 [3], L2009R2 cluster #13 appears to be an aggregate of grains that sample a diversity of solar and perhaps pre-solar environments. Sub-micron, grain by grain measurement of trace element contents and elemental oxidation states determined by XANES spectroscopy offers the possibility of understanding the environments in which these grains formed when compared to standard spectra. By comparing thermodynamic modeling of condensates with analytical data an understanding of transport mechanisms operating in the early solar system may be attained.

Acknowledgements: Thanks to Cyrena Goodrich for providing the urelite sample. This work was supported by NASA Cosmochemistry grant NNX10AJ17. The measurements were performed at the NSLS using the X26A microprobe funded by DoE Geosciences (DE-FG02-92ER14244). NSLS is funded by DoE.

References: [1] Ishii, H. A. et al. (2008) *Science*, 319,447 [2] Brownlee, D. et al. (1996) *ASP Conf. Series*, 104,261 [3] Thomas, K.L. et al. (1995) *Geochim cosmochim* 59,2797 [4] Messenger, S. et al. (2006) In: *Meteorites & Early Solar System II*, Univ. of Ariz Press [5] Zolensky, M. & Barrett, R. (1992), *MAPS*, 27R,312 [6] Bradley, J. (1994) *Geochim Cosmochim* 58,2123 [7] Keller, et al. (2004) *Geochim Cosmochim* 68, 2577 [8] Flynn, G., J. et al. (2012) *LPSC abstract #1089* [9] Brownlee, D.. (1994) *LPI Technical Report* 94-02,13 [10] Hadamcik, E., et al. (2009), *Plant. & Space Sci.* 57,1631 [11] Shafiq, M., et al. (2011), *Plant. & Space Sci.* 59, 17 [12] Stroud, R. M. (2005) *Astronomical Soc. Pacific Conf. Series* 341,645 [13]

Simon, S. B. et al., (2007) *Geochim Cosmochim* 71,
3098